Spectroscopic imaging ellipsometry for characterization of nanofilm pattern on Si substrate

Yonghong Meng (孟永宏)[1,2], She Chen (陈 涉)[1,2], and Gang Jin (靳 刚)[1*]

[1] *Key Laboratory of Microgravity (National Microgravity Laboratory), Institute of Mechanics, Chinese Academy of Sciences, Beijing 100190, China*

[2] *Graduate University of Chinese Academy of Sciences, Beijing 100049, China*

* *E-mail: gajin@imech.ac.cn*

Received November 20, 2009

Spectroscopic imaging ellipsometry (SIE) is used to characterize a nanofilm pattern on a solid substrate. The combination of a xenon lamp, a monochromator, and collimating optics is utilized to provide a probe beam with diameter of 25 mm, a charge-coupled device (CCD) camera with an imaging lens set and a lateral resolution in tens of microns is used as the detector. The sampling is approached by a rotating compensator at 8 seconds per wavelength. An 8–35-nm-thick stepped SiO_2 on Si substrate is characterized in the range of 400–700 nm with a thickness resolution of approximate 0.2 nm.

OCIS codes: 300.0300, 310.0310, 120.0120, 240.0240.

doi: 10.3788/COL201008S1.0114.

In recent decades, surface devices based on nanofilm patterns on Si substrates have been increasingly used in many fields, such as semiconductor integrated circuits, solar cells, and high-throughput biochips. In order to evaluate the performance of the film pattern, it is crucial to characterize the physical properties distribution with an appropriate lateral resolution, including dielectric function, film thickness, surface roughness, composition analysis, and so on.

Ellipsometry, which is based on the detection of probe beam change in polarization states before and after reflection upon a surface of a thin film specimen, has been well established as a powerful approach for characteristic of nanofilm in solid substrates[1,2]. This is advantageous because of its non-contact with specimens, non-destructiveness, sensitivity of atomic layer resolution, and lesser limitation for specimen materials. The basic measurement parameters in ellipsometry are the so-called ellipsometric angles ψ and Δ defined as

$$\rho = \frac{R_\mathrm{p}}{R_\mathrm{s}} = \tan\psi e^{j\Delta}, \qquad (1)$$

where R_p and R_s are the complex reflection coefficients of light polarized parts parallel and perpendicular to the plane of incidence, respectively, and ρ is the complex reflectance ratio.

Spectroscopic ellipsometry (SE), which drastically enhances the performance of ellipsometry with regard to spectral resolving capability, has developed into a practical standard approach to analyze multi-layered nanofilm. It obtains spectra of ellipsometric angles $\psi(\lambda)$ and $\Delta(\lambda)$ as function of wavelength from ultraviolet (UV) to infrared (IR), which can be processed by a numerical fitting program to provide physical and spatial properties of the specimen[3,4]. However, conventional SE can measure only one point at a time, and its lateral resolution is limited within the order of ~mm, generally because it utilizes a single light beam as probe and a single point photoelectric device as detector. In order to characterize a thin film pattern and analyze the specimen point by point, several SE systems based on mechanical scanning have been proposed[5,6]. However, the slow speed limits them from practical application for film patterns with large areas. A spectral imaging ellipsometer employing mono-axial spectrograph has also been proposed[7]. Such a device simultaneously measures spectroscopic ellipsometric angles, $\psi(\lambda, x)$ and $\Delta(\lambda, x)$, of one dimension of the sample; however, it still requires mechanical scanning along the perpendicular direction of the line for whole two-dimensional (2D) mapping. A practical solution to improve the measurement speed and lateral resolution for characterization of 2D nanofilm pattern is to enhance the detection performance of SE by using an optical imaging technique[8].

This work presents a spectroscopic imaging ellipsometer (SIE) for nanofilm pattern that utilizes the combination of a xenon lamp, a monochromator, and collimating optics to provide an expanded probe beam with the configuration: polarizer, compensator, specimen, and analyzer. A CCD camera with an imaging lens set is used as a detector for large area measurement. The sample is approached by a rotating compensator for quantitative measurement. The system is automatically controlled for easy use. A stepped SiO_2 on Si substrate is characterized in the range of 400–700 nm to show the functions of the SIE.

The diagram of the SIE setup is shown in Fig. 1. A 150-W xenon short arc lamp (OSRAM, Germany) operated by a supply (Newport, U.S.) with light ripple less than 0.5% regulation accuracy is used to provide a stable outgoing flux with continuous spectrum from IR to UV. In order to adequately utilize the light flux, an achromatic convergent lens set with a focal length of 200 mm and a diameter of 50 mm is used to converge the light beam into the entrance slit of a mechanical scanning grating monochromator (7-Star, China) with a focal length of 150 mm and an F-number of 1/4.5. The monochromator, under the control of the computer, provides a spectrum of 260–1600 nm with adjustable entrance and exit for

 © 2010 Chinese Optics Letters

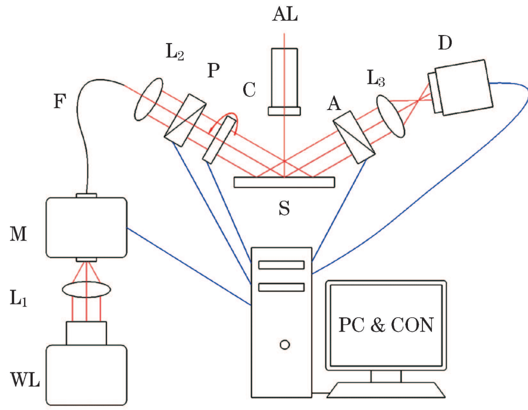

Fig. 1. Schematic of SIE system. WL: Xe lamp; L1, L2: achromatic lens set; M: scanning grating monochromator; F: optical fiber; P: polarizer; C: compensator; S: specimen; A: analyzer; AL: alignment telescope; L3: achromatic imaging lens set; D: CCD camera; PC and Con: computer and controller.

control of the light intensity and bandwidth, respectively. A glass optical fiber bound (Chunhui, China) by a spectrum of 380–1300 nm and a diameter of 1.0 mm is used to flexibly transfer the probe light from the exit of the monochromator to the focus point of the second achromatic convergent lens set. This collimates the single wavelength into an expanded probe beam with a diameter of 25 mm for nanofilm pattern detection at the same angle of incidence (AOI).

Two Glan-Taylor prisms (MELLES GRIOT, USA) with a spectral range of 250–2300 nm and an extinction ratio of 10^{-5} are used as the polarizer and the analyzer, respectively. A mica retardation plate (MELLES GRIOT, USA) with a spectral range of 400–700 nm is used as a compensator. Its phase retardation between fast axis and slow axis is near 90°, which is calibrated by a commercial V-VASE ellipsometer (J.A. Woollam, USA) and fitted by the Cauchy model. In order to adjust the azimuth with respect to the plane of incidence, the polarizer, compensator, and analyzer are fixed in hollow annular rotation stages driven by a servo motor (Newport, US) with a maximum speed of 40° per second and an absolute accuracy of 0.015°. The azimuths of the polarizing parts are calibrated by a self-calibrating method[9]. The specimen is fixed in the specimen stage by a vacuum pump with a linear-motor-driven free piston (NITTO KOHKI, Japan) and aligned by an optical self-collimated telescope (Micro-Radian, US).

An achromatic imaging lens set (Zesis, Germany) with a focal length of 50 mm and an F-number of 1.4 is used to image the specimen onto a scientific B/W video CCD camera (SONY, Japan). The camera features a corresponding spectrum range of 400–900 nm, sensitive area of 768 × 576 pixels on 6.0 × 4.96 (mm), and single pixel size of 6.5 × 6.25 (μm). The electronic gain is fixed for quantitative photonic intensity measurement. The sampling speed is 30 fps at maximum. The nonlinearity of the CCD camera is better than 1%. The image signal is inputted into an image grab board (Matrox, Canada) inserted in computer for analog-to-digital (A/D) conversion and digital image processing. The ellipsometric images are recorded in 8-bit (0–255) grayscale format. Image averaging method is used to improve the signal-to-noise ratio[10].

Among the sampling methods developed for quantitative measurement in ellipsometry[2], the rotating compensator method is utilized in the SIE due to several distinct advantages[11−13], such as non-ambiguous determination of ellipsometric angle Δ, insensitivity to source and detector polarization, no requirement of a direct current (DC) level, self-calibration, and so on.

The azimuth of the analyzer is preset at $+45^o$ or −45°, and the azimuth of the polarizer is preset at an optimum angle with respect to the incident plane to reduce systematic error. Under automatic control, the azimuth of the compensator is changed step by step with equal angle interval. At each sampling point of the azimuth of the compensator, an ellipsometric image is captured in grayscale, where the value of each pixel in grayscale corresponds to a micro-area on the specimen and takes the following form[11]:

$$\begin{aligned} S_n = {} & \alpha_0 + \alpha_{2c}\cos 2C_n + \alpha_{2s}\sin 2C_n \\ & + \alpha_{4c}\cos 4C_n + \alpha_{4s}\sin 4C_n, \end{aligned} \quad (2)$$

where C_n is the azimuth of the compensator of the sampling point. The coefficients α_{2c}–α_{4s} relating to the properties of the specimen are obtained by Fourier analysis of all the images captured at all sampling points under the present wavelength[11],

$$\begin{aligned} \alpha_{2c} &= \frac{2}{m}\sum_{n}^{m-1} S_n\cos 2C_n \\ \alpha_{2s} &= \frac{2}{m}\sum_{n}^{m-1} S_n\sin 2C_n \\ \alpha_{4c} &= \frac{2}{m}\sum_{n}^{m-1} S_n\cos 4C_n \\ \alpha_{4s} &= \frac{2}{m}\sum_{n}^{m-1} S_n\sin 4C_n, \end{aligned} \quad (3)$$

where m is the number of sampling point. In order to deduce ellipsometric parameters properly, the equal angle interval should be no less than 22.5°. The ellipsometric angles $\psi(x, y)$ and $\Delta(x, y)$ under the present wavelength of each corresponding micro-area on the specimen can then be achieved by[14]

$$\tan 2\psi = \frac{\sqrt{(\alpha_{2s}^2+\alpha_{2c}^2)\tan^2\frac{\delta_C}{2} + 4\left(\alpha_{4s}\cos 2P - \alpha_{4c}\sin 2P\right)^2}}{-2\left(\alpha_{4c}\cos 2P + \alpha_{4s}\sin 2P\right)},$$

$$\tan\Delta = \frac{1}{2}\tan\left(\frac{\delta_C}{2}\right)\frac{\alpha_{2c}\sin 2P - \alpha_{2s}\cos 2P}{\alpha_{4c}\sin 2P - \alpha_{4s}\cos 2P}, \quad (4)$$

where δC is the phase retardation of the compensator between fast and slow axes and P is the azimuth of the polarizer.

The spectroscopic ellipsometric angles, $\psi(\lambda, x, y)$ and $\Delta(\lambda, x, y)$, in full spectrum can be achieved with wavelength scanning of the monochromator. Furthermore, physical properties in pixel lateral resolution of the specimen, such as film thickness distribution, refraction index, etc., can be deduced by a fitting procedure. In order to evaluate the fitting degree of model data and the experimental data, the minimum square error (MSE) function

is used by[3]

$$\mathrm{MSE}=\frac{1}{2N-M}\sum_{i=1}^{N}\left[\left(\frac{\psi_i^{\mathrm{mod}}-\psi_i^{\mathrm{exp}}}{\sigma_{\psi,i}^{\mathrm{exp}}}\right)^2+\left(\frac{\Delta_i^{\mathrm{mod}}-\Delta_i^{\mathrm{exp}}}{\sigma_{\Delta,i}^{\mathrm{exp}}}\right)^2\right], \quad (5)$$

where N is the number of ellipsometric angles set (ψ, Δ), M is the number of the fitting parameters, σ is the standard error of experimental data (ψ, Δ), and (ψ^{mod}, Δ^{mod}) and (ψ^{exp}, Δ^{exp}) are ellipsometric angles set of model and experiment, respectively. The MSE should be minimized during the fitting process.

In order to eliminate the system error resulting from the azimuth deviation and imperfect optics components of the polarizing parts (the polarizer, compensator, and analyzer), as well as the phase retardation error of the compensator, the two-zone averaging method is used. The technique averages the results obtained when azimuth of analyzer is set at +45° or –45°[14]. Other measures, including multi-image averaging and additional sampling points, are taken in order to decrease the random error resulting from the intensity fluctuation of the probe beam, photo-electrical noise of the imaging sensor, background light, the angle interval between two sampling points, and so on.

The SIE system is automatically controlled by a computer, including hardware motion control, image acquisition, and data process under the operation of the system software[15,16].

The major motion functions include system initialization (e.g., specimen fixing and self-calibration), system setting (e.g., azimuth setting), magnification adjustment according to the size of the specimen and the lateral resolution, AOI adjustment, auto-focusing, wavelength scanning, and positioning for the feedback of the location of the moving parts.

Image acquisition functions mainly include image capture upon requirement (e.g., number of frames, the time interval, average of multi-images, and so on) and image processing (e.g., choice of an interesting special area, readout of the value in grayscale in the area, image transfer to 3D, and so on).

Data processing mainly includes Fourier analysis to obtain coefficients $\alpha_{2c}-\alpha_{4s}$ in Eq. (3), ellipsometric angles $\psi(\lambda, x, y)$ and $\Delta(\lambda, x, y)$ of each micro-area of the specimen corresponding to a pixel of an image, and the deduction for the properties of the specimen such as the thickness and distribution of the thin film and the refraction index.

Some experimental results obtained with the SIE system are presented. The specimen (Fig. 2) is a Si substrate with stepped SiO_2 layer with 18.27 (H) × 3.69 (V) (mm) in size and consisting of four layers with different SiO_2 thicknesses between 8 and 35 nm. It is prepared by eroding the SiO_2 layer with a thickness of 65 nm on Si with hydrofluoric acid under a controlled time.

The AOI is set at 70°, which is near the Brewster angle of the silicon substrate. An optical magnification of 0.254 is fixed in order to image the whole specimen. The specimen size image is 300 (H) × 150 (V) pixels, and the corresponding lateral resolution is 60.9 (H) × 24.6 (V) (μm) in the parallel and perpendicular direction with respect to the incident plane. The spectral range of 400–700 nm is chosen and the wavelength interval of 50 nm is set, due to the smooth change in the refraction indexes of SiO_2 and Si in the spectrum. The wavelength bandwidth is set at 9.9 nm. Under this condition, the sampling time under each wavelength is 8 s.

Eight raw images in grayscale recorded under the condition of AOI=70°, λ=500 nm, P=0°, A=45°, C=11.25° (a), 33.75° (b), 56.25° (c), 78.75° (d), 101.25° (e), 123.75° (f), 146.25° (g), and 168.25° (h) are shown Fig. 2. The four layers and their boundaries can be distinguished easily from the image because the slight difference in the thickness of SiO_2 layer on Si leads to a big difference in phase modulation, which is the basis of ellipsometry. The value difference of the same layer in grayscale, which depends on the azimuth of compensator, indicates the specimen response to the incoming polarizing state of probe beam. The rectangles denoted by A, B, C, and D are the selected areas with top-left positions (x, y) in pixel A (x = 30, y=74), B (x=110, y=69), C (x=201, y=64), and D (x=283, y=57). Each area in image consists of 12 × 12 pixels, and their corresponding area in film pattern is 0.731 (H) × 0.295 (V) (mm).

The ellipsometric angles image, $\psi(\lambda$=500 nm, x, y) and $\Delta(\lambda$=500 nm, x, y), of the thin film pattern derived by using the two-zone averaging method, which is deduced by analysis of all the images obtained at each sampling point under the wavelength, are shown in Fig. 3. It can be seen that the ellipsometric angles distribution varies slightly within each layer and changes abruptly between each two-step, which indicates that the abrupt variation properties of this area are mainly due to the SiO_2 thickness variation. The abnormal jump down in the boundaries between each two adjoining layers mainly results from the sample preparation pro-

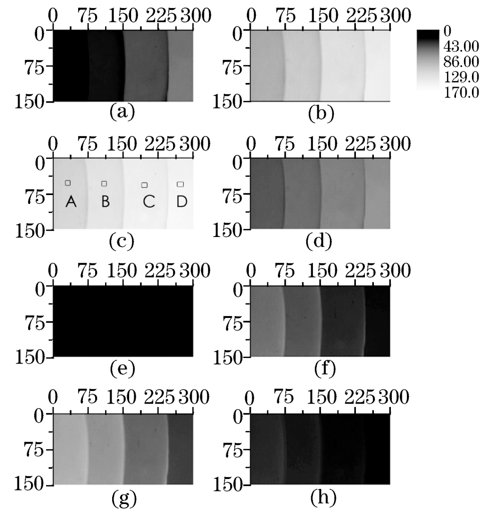

Fig. 2. Raw images in grayscale with a size of 300 × 150 pixels captured at AOI=70°, λ=500 nm, P=0°, A=45°, C= 11.25° (a), 33.75° (b), 56.25° (c), 78.75° (d), 101.25° (e), 123.75° (f), 146.25° (g), and 168.25° (h). The rectangle denoted by A, B, C, and D are selected areas with top-left positions (x, y) in pixel are A (x=30, y=74), B (x=110, y=69), C (x=201, y=64), and D (x=283, y=57), respectively. Each area consists of 12 × 12 pixels and their corresponding area in film pattern is 0.731 (H) × 0.295 (V) (mm).

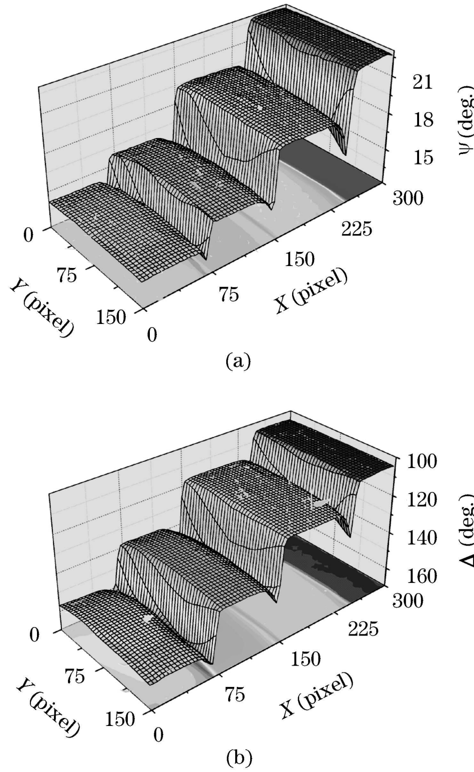

Fig. 3. Ellipsometric angles distribution of (a) $\psi(\lambda=500$ nm, x, $y)$ and (b) $\Delta(\lambda=500$ nm, x, $y)$ of SiO_2/Si at AOI=70°, λ=500 nm.

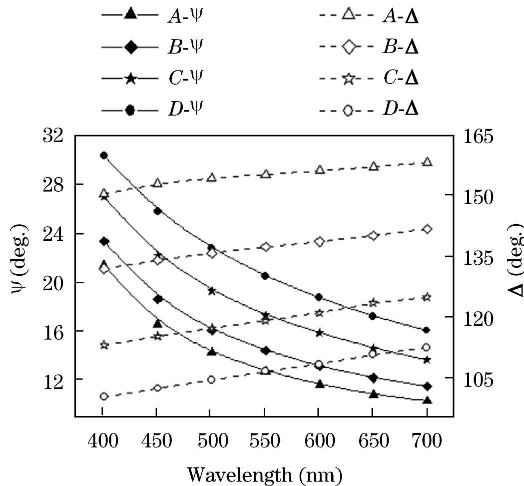

Fig. 4. Spectroscopic ellipsometric angles $\psi(\lambda, x, y)$ and $\Delta(\lambda, x, y)$ of selected areas A, B, C, and D, shown in Fig. 2. AOI=70°, λ =400–700 nm.

cedure when hydrofluoric acid solution sways and makes the boundaries rough and irregular.

By using wavelength scanning, spectral ellipsometric angles images, $\psi(\lambda, x, y)$ and $\Delta(\lambda, x, y)$, of each micro-area over the entire film pattern of view can be achieved simultaneously. Figure 4 shows the spectroscopic ellipsometric angles $\psi(\lambda, x, y)$ and $\Delta(\lambda, x, y)$ of four individual areas, A, B, C, and D, as shown in Fig. 2, within the range of 400–700 nm. The $\psi(\lambda, x, y)$ and $\Delta(\lambda, x, y)$ are the average values of the corresponding areas. It can be seen that the ellipsometric angles of each area change smoothly, and the difference between two adjoining layers is distinguished very clearly. In order to deduce the unknown thickness of the selected area, the physical model of air-SiO_2-Si is used to describe the film pattern, and the fitting procedure is carried out with the WVASE 32 Software (J. A. Woollam, US). The fitting thicknesses of areas, A, B, C, and D, are listed in Table 1. It can be concluded that the physical model is appropriate and that the thickness resolution is approximately 0.2 nm.

Table 1. Fitting Thickness of SiO_2 Selected Area A, B, C, and D Using WVASE32 Software and the Physical Model Air-SiO_2-Si

Selected Area	A	B	C	D
Fitting Thickness (nm)	8.18±0.09	15.5±0.1	25.3±0.2	34.6±0.2
MSE	1.040	0.846	1.382	1.854

In conclusion, a SIE method is used to characterize the physical properties of a nanofilm pattern in terms of the dielectric function, film thickness, surface roughness, composition analysis, and so on. It utilizes the xenon lamp, monochromator, and collimating optics to provide a probe beam with a diameter of 25 mm combined with the polarizer, compensator, specimen, and analyzer. The CCD camera with an imaging lens is used for large area detection. A rotating compensator method is applied for quantitative sampling. The greatest advantage of the SIE is that it can achieve the spectroscopic parameters, $\psi(\lambda, x, y)$ and $\Delta(\lambda, x, y)$, of a nanofilm pattern on solid substrate with optical lateral resolution in the order of wavelengths. Under the present automatic setup, the 8–35-nm-thick stepped SiO_2 on Si with size of 18.27 (H) $\times$ 3.69 (V) (mm) is characterized at the spectrum region of 400–700 nm with the lateral resolution 60.9×24.6 (μm) in the parallel and perpendicular directions with respect to the plane of incidence. The sampling speed is faster than 8 s per wavelength with images of 768×576 pixels. Further fitting analysis by the use of the model air-SiO_2-Si indicates that the thickness resolution is approximately 0.2 nm.

This work was supported by the Chinese Academy of Sciences (Nos. YZ0629 and KJCX2.YW.M03), the National "863" Program of China (No. 2008AA02Z419), and the National "973" Program of China (No. 2009CB320302).

References

1. R. M. A. Azzam and N. M. Bashara, *Ellipsometry and Polarized Light* (North-Holland, Amsterdam, 1977).
2. H. G. Tompkins and E. A. Irene, Handbook of ellipsometry (William Andrew Inc., New York, 2005).
3. K. Vedam, Thin Solid Films **313-314,** 1 (1998).
4. H. Fukiwara, Spectroscopic Ellipsometry: Principles and Applications (John Wiley & Sons, 2007).
5. M. Erman and J. B. Theeten, J. Appl. Phys. **69,** 859 (1986).
6. L. M. Karlsson, M. Schubert, N. Ashkenov, and H. Arwin, Phys. Stat. Sol. (c) **2,** 3293 (2005).
7. W. Chegal, Y. J. Cho, H. J. Kim, H. M. Cho, Y. W. Lee, S. H. Kim, Jpn . J. Appl. Phys. **43,** 6475 (2004).
8. A. J. Choi, T. J. Kim, Y. D. Kim, J. H. Oh, and J. Jang, J. Korean Phys. Soc. **48,** 1544 (2006).

9. I. An, J. A. Zapien, C. Chen, A. S. Ferlauto, A. S. Lawrence and R. W. Collins, Thin solid films **455-456,** 132 (2004).
10. Y. Meng and G. Jin, Opt. Prec. Eng. **8,** 316 (2000).
11. P. S. Hauge and F. H. Dill, Opt. Commun. **14,** 431 (1975).
12. J. Lee, P. I. Rovira, Ilsin An, and R. W. Collins, Rev. Sci. Instrum. **69,** 1800 (1998).
13. D. E. Aspnes, J. Opt. Soc. Am. A **21,** 403 (2004).
14. R. Kleim, L. Kuntzler, and A. Elghemmaz, J. Opt. Soc. Am. A **11,** 2550 (1994).
15. Y. H. Meng, S. Chen, and G. Jin, Phys. Stat. Sol. (c) **5,** 1046 (2008).
16. Y. H. Meng, Y. Y. Chen, C. Qi, L. Liu, and G. Jin, Phys. Stat. Sol. (c) **5,** 1050 (2008).